On the characteristics of air layer regimes

Nikolaidou, Lina; Laskari, A.; van Terwisga, T.J.C.; Poelma, C.

Publication date
2021

Document Version
Final published version

Published in
11th International Symposium on Cavitation (CAV2021)

CAV2021
11th International Symposium on Cavitation
May 9-13, 2021, Daejon, Korea

On the characteristics of air layer regimes

Lina Nikolaidou[1*], Angeliki Laskari[1], Tom van Terwisga[2,3], Christian Poelma[1]
[1]Process and Energy, Delft University of Technology, Netherlands
[2]Maritime and Transport Technology, Delft University of Technology, Netherlands
[3]Maritime Research Institute of the Netherlands (MARIN), Netherlands

Abstract: Different air layer regimes were created experimentally beneath a flat plate without the use of a backwards facing step or a cavitator. The effect of the free-stream velocity and the air flow rate on the air layer formation and the regime transitions was characterized using the percentage of non-wetted area for each condition. While other researchers classify regimes based on drag reduction here the focus is to quantify the air layer regimes using the distribution of wetted/non-wetted areas and define the different air layer regimes accordingly. Post-processing of images of air layer regimes shows that the percentage of non-wetted area increases with increasing air flow rate in the bubbly and transitional regime, while in the stable air layer regime the percentage of non-wetted area is almost independent of the air flow rate. Increasing the free-stream velocity leads to an increase of the critical air flow rate and a delayed transition from the bubbly regime to the air layer regime. Results of this study are expected to be utilized in drag reduction by air lubrication studies.

Keywords: air layer; non-wetted area; regime transition;

1. Introduction

Friction drag accounts on average for approximately 70% of the overall resistance of a ship [1], and thus a large part of a typical ship's propulsive power is required to overcome the friction drag. To reduce this drag, air layer lubrication techniques, among other methods, have been proposed and investigated over the past years. Those methods could lead to savings in fuel costs and a lower environmental impact. In most studies on drag reduction by air lubrication, a cavitator or backward-facing step (BFS) is used upstream of the air injection [2, 3, 4, 5]. In this work, an air layer is created beneath a flat plate without the use of a cavitator or BFS. This case demands the least amount of modifications on existing ships and thus poses less obstacles to the implementation of such methods. For this configuration, three different air layer regimes are commonly observed (Figure 1); the bubble drag reduction (BDR) regime, characterized by the presence of dispersed bubbles in the flow, the air layer drag reduction (ALDR) regime where a continuous air layer is formed, and the transitional air layer drag reduction (TALDR) regime, where alternating regions of bubbly flow and segments of air layer are present. According to the definitions introduced by Elbing et al. [6], once a drag reduction of 20% is achieved the transitional regime is reached, while a drag reduction of $> 80\%$ marks the air layer drag reduction regime. The latter one is the most efficient in drag reduction [3], but the sea state, trim and motion of the ship, the flow field around the hull, piping losses, and other factors contribute to the possibility of a transitional, rather an ALDR [7]. In the present study, the focus is on evaluating the effect of different free-stream velocities and air flow rates on the air layer formation and regime transitions. In doing so, a method is proposed for characterizing the different regimes based on the distribution of wetted and non-wetted areas. This would provide an alternative to the need of drag force measurements to characterize the air layer regimes. In addition, quantifying the non-wetted area under different air flow rates and free-stream velocities could provide insight in the bubble/air-layer break-up, bubble coalescence and bubble size distribution. The aforementioned phenomena contribute to (or inhibit) the transition from bubbly regime to the desired air layer regime.

* Corresponding Author: Lina Nikolaidou, M.Nikolaidou@tudelft.com

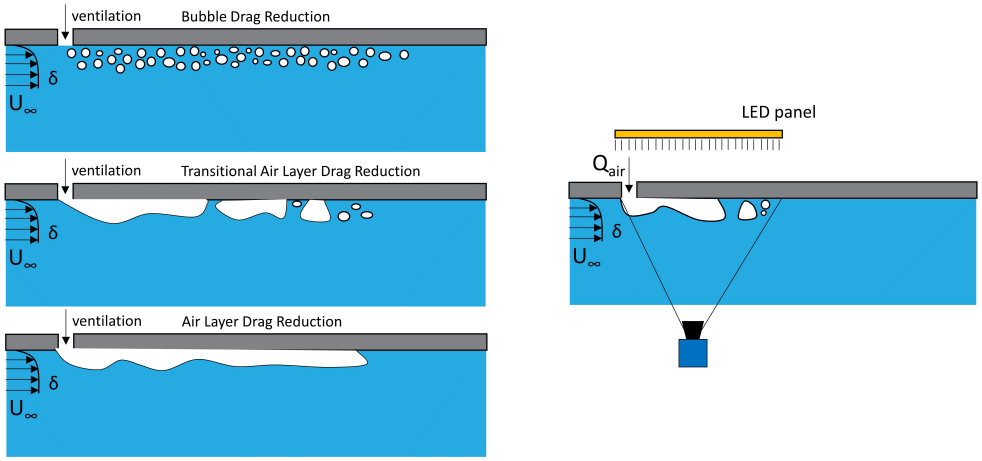

Figure 1: Schematic representation of the different air layer regimes (left) and experimental setup (right).

2. Experimental Setup and Methods

Experiments were performed in the water tunnel of the Laboratory for Aero & Hydrodynamics of the Delft University of Technology. The test section of the tunnel has a cross-sectional area of 60 x 60 cm^2 and a length of 5 m. The open surface of the water tunnel was covered with two identical flat plates, each 2.485 m long, tightly placed one after the other. The water depth was d = 58 cm. The downstream plate was modified to accommodate the air injection; air was injected through a spanwise slot, 50 cm downstream of the leading edge of the plate. Each plate was equipped with side fences, to prevent the air from escaping through the sides. The available development length before the air injection (3.5 m) was chosen such that the incoming boundary layer thickness is maximized, while also allowing sufficient downstream length for the air layer formation and therefore a better comparison with the full-scale case. A slot type injector was fitted, spanning the central 58 cm of the downstream plate width. The width of the slot was 4 mm. Compressed air was injected from the top side of the plate through two manifolds and dispersed over the width of the slot. No backwards facing step or cavitator was used on the upstream edge of the injector. The air flow rate, Q_{air}, was manually controlled with a valve and measured with a rotameter. A pitot-static tube was placed at the downstream end of the test section to measure the free-stream velocity, U_∞. The objective was to explore the different air layer regimes and how they vary with U_∞ and air flow rate Q_{air}. For that purpose, for each free-stream velocity, Q_{air} was varied from 0 to 52 l/min. The tested free-stream velocities ranged from 0.68 m/s to 0.94 m/s with a Reynolds number based on the water depth, Re_d ranging from 3.94×10^5 to 5.45×10^5. The Reynolds number based on the downstream distance Re_x ranged from 2.4×10^6 to 3.3×10^6. Planar PIV was used upstream of the injector in a side-view configuration to characterize the incoming boundary layer. The boundary layer thickness δ_{99} was estimated to be around 70 mm. Images of the air layer regimes were acquired with a bottom up view (Figure 1). The different air layer regimes were imaged with LaVision's Imager sCMOS CLHS camera, fitted with a f/2.8D AF Micro Nikkor lens (24 mm). On the upper surface of the downstream plate an LED panel provided background illumination. The camera exposure time δt was 3 ms and the image acquisition rate was 2 Hz. The field of view was approximately

* Corresponding Author: Lina Nikolaidou, M.Nikolaidou@tudelft.com

700 x 600 mm^2 and the magnification approximately 3.6 px/mm in both directions. For each measurement set, 1500 uncorrelated images were acquired.

To characterize the air layer regimes under different U_∞ and Q_{air}, the non-wetted area of each image is calculated. Within a grayscale image, large intensity gradients are present in the air-water interface. Based on the magnitude of these intensity gradients, a threshold is applied and the grayscale image is binarized. Subsequently, small structures are removed and morphological closing (dilation followed by an erosion) is performed and the remaining bubbles/air patches are filled. A binary image is then formed indicating wetted and non-wetted areas. The non-wetted area is normalized with the total area of interest. The result is averaged over the total number of images acquired for each combination of U_∞ and Q_{air}.

3. Results & Discussion

Typical images of the air layer regimes for free-stream velocities of 0.77 m/s and 0.94 m/s are shown in Figure 2. For each flow velocity, characteristic air layer regimes are shown for air flow rates of 10.3 l/min (Figures 2a, 2d), 15.5 l/min (Figures 2b, 2e) and 52 l/min (Figures 2c, 2f). It must be noted that except for the flow velocities all other parameters are kept constant. This is important since the incoming boundary layer characteristics and the air injection method also affect the creation of air layer regimes as observed in previous studies [6]. In both Figures 2a and 2d, a bubbly regime is depicted. For the lower velocity (Figure 2a) bubbles and air patches of the order of cm are present, while the bubbly flow of the higher velocity (Figure 2d) consists of smaller bubbles. For the intermediate air flow rate (Figures 2b, 2e), in the case of the higher velocity (Figure 2e), bubbles and air patches are now present in the flow, similar to the bubbly regime of Figure 2a. For the lower velocity, a quite different regime is observed. In this regime bubbles and air patches coalesce to form an elongated, highly dynamic air layer. In this transitional regime, bubbles and air patches continuously pinch-off the tip of the air layer. Further increasing the air flow rate, results in a stable but shorter air layer depicted in Figure 2c. In this regime air is entrained from the cavity mainly from the sides. A similar regime is also observed in Figure 2f, but with a longer cavity length. In this case air is entrained also from the middle of the cavity.

To characterize the effect of the air flow rate and the free-stream velocity on the air layer regimes, the normalized non—wetted area, A_{nw} is calculated for each [Q_{air}, U_∞] pair. This is defined as:

$$A_{nw} = \frac{A_{air}}{A_{total}} x100 \tag{1}$$

where A_{air} is the plate area covered by air and A_{total} is the total plate area.

The normalized non-wetted area versus air flow rate for four different velocities is shown in Figure 3a. Initially, increasing the air flow rate results in an increase of the non-wetted area for all velocities. This is evident also from Figure 3b, where the non-wetted area is normalized by its maximum (data below 0.5 in Figure 3b). This stage corresponds to a bubbly regime (Figure 2d), where an increase in the air flow rate results in larger bubbles and/or air patches. Further increasing the air flow rate results in an abrupt increase of the non-wetted area (transitional regime in Figure 2b). This is evident for flow velocities 0.77 m/s, 0.87 m/s and 0.94 m/s (Figure 3a). For the case of 0.68 m/s free-stream velocity, a similar behavior was observed between 5.15 l/min and 10.3 l/min air flow rates during the experiments, but it could not be measured due

* Corresponding Author: Lina Nikolaidou, M.Nikolaidou@tudelft.com

to the limited sensitivity of the rotameter used. For all the velocities, the maximum non-wetted area $A_{nw,max}$ is observed in the transitional regime. This effect seems to diminish however for increasing free-stream velocities, which were limited here by the facility used. Higher velocities are planned for further investigation in the near future. Further increasing the air flow rate, results in a decrease of the non-wetted area and the stable air layer regime is reached. Once this air layer regime is reached, further increasing the air flow rate has no effect on the non-wetted area (asymptotic region in Figure 3a). The excess air is entrained from the sides of the air cavity in a higher rate. Previous studies concerning air cavities formed behind a BFS [3] have indicated that for a given free-stream velocity and water depth, there is a maximum and stable cavity length equal to one half of the gravity wavelength. Comparing the thickness of the air layer in our experiments with half a gravity wavelength, it is observed that there is a 5% and 10% difference for the two lower velocities, while for the higher velocities the difference is larger. Since in our setup air is injected vertically into the flow, it is hypothesized that this acts like a cavitator for the lower velocities and thus a better agreement in the cavity length is observed. Finally, the errorbars in Figure 3a represent two standard deviations, to show the variability in the wetted area between images. It can be seen that the standard deviation of the non-wetted area is larger in the transitional regime, because of the highly dynamic character of the air layer in this regime.

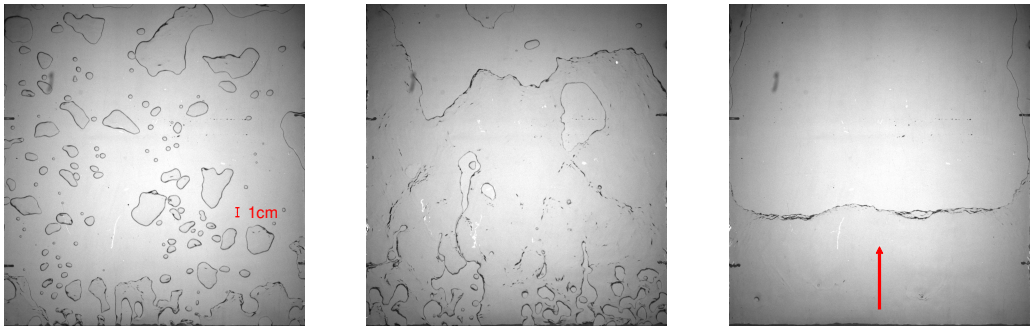

(a) U_∞ = 0.77 m/s & Q_{air} = 10.3 l/min

(b) U_∞ = 0.77 m/s & Q_{air} = 15.5 l/min

(c) U_∞ = 0.77 m/s & Q_{air} = 52 l/min

(d) U_∞ = 0.94 m/s & Q_{air} = 10.3 l/min

(e) U_∞ = 0.94 m/s & Q_{air} = 15.5 l/min

(f) U_∞ = 0.94 m/s & Q_{air} = 52 l/min

Figure 2: Characteristic images of air layer regimes for free-stream velocities U_∞ 0.77 m/s and 0.94 m/s. Flow direction is from down up.

* Corresponding Author: Lina Nikolaidou, M.Nikolaidou@tudelft.com

It can be seen from Figure 3a that qualitatively a similar behavior is observed in all the tested free-stream velocities with only a shift towards higher air flow rates for increasing velocities. This is made more clear in Figure 4a, where the transitional and the critical air flow rates for each free-stream velocities are shown. As expected, the transitional and critical air flow rates increase with increasing free-stream velocity. This effect was first indicated by Elbing et al. [6]. In Figure 4b the air flux is made non-dimensional with $U_\infty A_{slot}$, with A_{slot} being the outflow area of the air injector. Similar to Figure 4a, it can be seen that the critical air flow rate Q_{air} is approximately proportional to the square of the free-stream velocity.

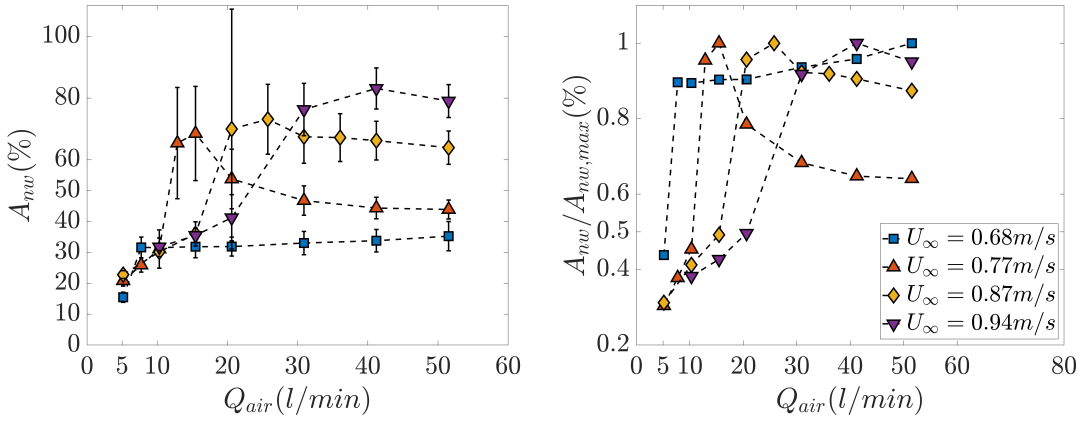

(a) (b)

Figure 3: Percentage of non-wetted area versus air flow rate for different free-stream velocities (a) and normalized percentage of non-wetted area versus air flow rate (b).

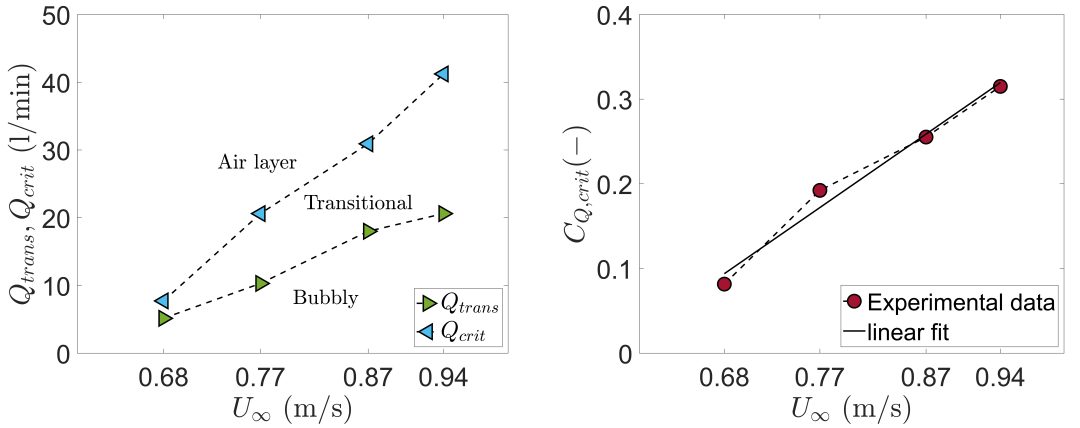

(a) (b)

Figure 4: Transitional and critical air flow rates for different free-stream velocities (a) and non-dimensional air flow rate $C_Q = \dfrac{Q_{air}}{U_\infty A_{slot}}$ for different free-stream velocities(b).

* Corresponding Author: Lina Nikolaidou, M.Nikolaidou@tudelft.com

It can be argued that since the transitional regime exhibits larger non-wetted area coverage than the air layer regime, design conditions for air lubrication systems in ships should be realized for this and not for the air layer regime. However, the transitional regime is an unstable one and small perturbations (due to e.g. sea state, the ship motion) could more easily lead to the bubbly regime. In contrast, the air layer regime is a stable regime and once it is reached, small perturbations do not affect its formation.

4. Conclusions:

Different air layer regimes were created experimentally beneath a flat plate and the effect of free-stream velocity and air flow rate was illustrated. The characterization of the different regimes was done via the percentage of non-wetted area, decoupled from drag reduction estimates. For a given velocity the percentage of non-wetted area increases for increasing air flow rates in the bubbly and transitional regime and decreases in the air layer regime. Once the air layer regime is reached, further increasing the air flow rate has no effect on the stability and the cavity length. Increasing the free-stream velocity results in an increase on the transitional and critical air flow rate. Future experiments are planned to investigate the influence of the incoming boundary layer characteristics on the transition (defined as percentage of non-wetted area). This is expected to be particularly important in the absence of a cavitator or BFS upstream of the air injector.

Acknowledgements: This work is part of the public–private research program "Water Quality in Maritime Hydrodynamics" (AQUA) project P17-07. The support by the Netherlands Organisation for Scientific Research (NWO) Domain Applied and Engineering Sciences, and project partners is gratefully acknowledged.

5. References:

[1] Lars Larsson. Ship resistance and flow. *Published by The Society of Naval Architects and Marine Engineers, SNAME, The Principles of Naval Architecture Series, ISBN: 978-0-939773-76-3*, 2010.

[2] Brian R Elbing, Simo Mäkiharju, Andrew Wiggins, Marc Perlin, David R Dowling, and Steven L Ceccio. On the scaling of air layer drag reduction. *Journal of fluid mechanics*, 717:484–513, 2013.

[3] Oleksandr Zverkhovskyi. *Ship drag reduction by air cavities*. PhD thesis, TU Delft, 2014.

[4] D Kim and P Moin. Direct numerical study of air layer drag reduction phenomenon over a backward-facing step. *Center for Turbulence Research, Annual Research Briefs*, pages 351–363, 2010.

[5] BW Pearce, PA Brandner, and SJ Foster. Ventilated cavity flow over a backward-facing step. In *Journal of Physics: Conference Series*, volume 656, page 012164. IOP Publishing, 2015.

[6] Brian R Elbing, Eric S Winkel, Keary A Lay, Steven L Ceccio, David R Dowling, and Marc Perlin. Bubble-induced skin-friction drag reduction and the abrupt transition to air-layer drag reduction. *Journal of Fluid Mechanics*, 612:201–236, 2008.

[7] Simo A Mäkiharju, Marc Perlin, and Steven L Ceccio. On the energy economics of air lubrication drag reduction. *International Journal of Naval Architecture and Ocean Engineering*, 4(4):412–422, 2012.

* Corresponding Author: Lina Nikolaidou, M.Nikolaidou@tudelft.com